Hindawi
Geofluids
Volume 2022, Article ID 7438074, 13 pages
https://doi.org/10.1155/2022/7438074

Research Article

Effect of Microscopic Pore Throat Structure on Displacement Characteristics of Lacustrine Low Permeability Sandstone: A Case Study of Chang 6 Reservoir in Wuqi Oilfield, Ordos Basin

Ren Qiang,[1] **Wei Hu**,[2] **Lei Guofa**,[3] **Zhang Weigang**,[4] **Ge Bingyu**,[5] **and Nan Junxiang**[6]

[1]*School of Geology Engineering and Geomatics, Chang'an University, Xi'an, 710054, China*
[2]*Research Institute of Shaanxi Yanchang Petroleum (Group) Co., Ltd., Xi'an, Shaanxi 710075, China*
[3]*No.5 Gas Production Plant, Changqing Oilfield Company, PetroChina, Wushenqi, 017300, China*
[4]*No.8 Oil Recovery Plant of PetroChina Changqing Oilfield Company, Xi'an, Shaanxi 710201, China*
[5]*No.1 Gas Production Plant, Changqing Oilfield Company, PetroChina, Jingbian, 718500, China*
[6]*Research Institute of Exploration and Development, PetroChina Changqing Oilfield Company, Xi'an, 710018, China*

Correspondence should be addressed to Ren Qiang; 2018026003@chd.edu.cn

Received 17 June 2022; Accepted 19 September 2022; Published 13 October 2022

Academic Editor: Wenhui Li

Pore throat structure is the key factor affecting displacement efficiency in low permeability reservoirs. In this paper, the pore throat structure and displacement characteristics of Chang 6 low permeability sandstone reservoir in Wuqi area of Ordos Basin were studied by casting thin section analysis, scanning electron microscopy, XRD, high-pressure mercury injection, and microscopic displacement model of real sandstone test. The results show that the size and homogeneity of the pore throat structure deteriorate gradually from type I to type IV reservoir, and the corresponding displacement efficiency also decreases gradually. The type I reservoir is dominated by uniform displacement, and residual oil is dominated by oil film. Type II reservoir is dominated by mesh and finger displacement, while type III reservoir is dominated by finger displacement, and continuous remaining oil distribution is easy to be formed after water flooding. Pore throat size and homogeneity are important factors affecting oil displacement efficiency. The larger the pore throat size, the more homogeneous the structure, and the stronger the seepage capacity, the higher the oil displacement efficiency. With the increase of volume displacement multiple, the displacement efficiency growth rate of the type I reservoir changes little, while the displacement efficiency growth rate of the type II and type III reservoir decreases gradually. In actual production and development, reasonable control of pressure is the key to dependable production.

1. Introduction

The exploration and development of low permeability sandstone oil and gas in unconventional reservoirs play a significant position in China's oil and gas field [1–4]. In China, the Yanchang Formation in the Ordos Basin is famous for its low permeability sandstone oil reservoirs [5–7]. The pore throat structure of low permeability sandstone is relatively complex compared to conventional reservoirs, and micro-nano-scale pore throats are mainly developed [8–12], resulting in difficult flow capacity and low recovery. Controlled by the pore throat structure, the migration law of oil and water phases at the microstructure and pore scale of the reservoir is complex, and the macroscopic production laws are unclear [13–16]. It is the basis of enhancing oil recovery of low permeability reservoirs to clarify pore throat structure characteristics and the effect of different pore throat structures on oil and water phase migration characteristics [17–20]. With the innovation of electron microscope technology in recent years [21–23], more and more attention has been paid to the micropore throat structure and water displacement path. It is believed that the microscopic pore structure of the low permeability reservoir restricts the water displacement characteristics [24, 25], and the characteristics

of water displacement in different pore throat structures are obviously different.

The study area is located in the mid-west of Yishan slope in the Ordos Basin, which is composed of six secondary tectonic units (Figure 1) [26]. The Triassic Yanchang Formation is divided into 10 oil layer groups from bottom to top [27]. Among them, the Chang 6 oil group is the main oil-producing layer in this area. A typical lake-delta sedimentary system developed in Chang 6 period, and the underwater distributary channel is the main reservoir space, which showed typical low permeability characteristics [26, 27]. The complex pore throat structure of the low permeability reservoir further results in an unclear fluid flow law.

In order to clarify the water displacement characteristics of different pore structure types, experimental test methods such as high-pressure mercury intrusion (HPMI), cast thin sections (CTS), XRD, and scanning electron microscopy (SEM) were used to study the pore throat structure. And the characteristics of water displacement of different pore throat structures were studied by the microscopic displacement model of real sandstone test; further, the key influencing factors of the water displacement efficiency were analyzed. This paper is aimed at studying the pore throat structure characteristics of low permeability reservoir and identifying the displacement characteristics of different pore throat structures, so as to know the development of low permeability reservoir.

2. Experimental Methodology

2.1. HPMI. The high-pressure mercury intrusion (HPMI) experiment is considered the most effective method to clarify the pore throat structure characteristics of unconventional reservoirs. Nonwetting phase mercury is injected into the pores of the samples, and pressure and mercury saturation were recorded. The corresponding pore throat radius can be obtained based on the capillary pressure formula [28–30]. At present, the characterization of pore throat structure in low permeability reservoir by HPMI has been widely recognized by scholars. The curve shape of HPMI can not only reflect the size of pore throat but also represent the homogeneity of the pore throat structure [31, 32]. AutoPoreIV9510 automatic mercury injection instrument from Mac Inc. was used in this paper, the maximum working pressure of the instrument is 200 MPa, and the measurement range of pore throat radius is 0.003–1000 μm.

2.2. Microscopic Displacement Model of Real Sandstone. The microscopic displacement model of real sandstone records the migration path of oil and water and displacement efficiency by simulating the real water displacement process [18]. Firstly, the core samples were made into a thin slice of about 2.5 cm × 2.5 cm × 0.05 cm. According to the viscosity of crude oil and the salinity of formation water in the study area, the fluids simulating crude oil and formation water were prepared, and the colorants were added to dye red and blue, respectively, to facilitate the distinction under the electron microscope. By simulating the process of water displacement and increasing the pressure, the seepage path and displacement efficiency of oil and water in the microscopic pore structure of samples were observed by using an electron microscope and microscopic image acquisition technology, so the characteristics of oil and water transport were directly reflected. The displacement process was carried out in the State Key Laboratory of Continental Dynamics, Northwest University, using real sandstone microscopic water flooding experiment equipment.

2.3. Samples. The samples were collected from the low permeability sandstone of Yanchang Formation in Wuqi Oilfield and developed in delta front subfacies deposition. The results of casting thin section and scanning electron microscope show that the samples are mainly composed of feldspar sandstone and lithic feldspar sandstone. The average content of quartz was 27.1%, the average content of feldspar was 56.5%, and the lithic content has an average of 16.4% (Figures 2(a) and 2(b)). The porosity of 72 samples ranges from 2.99% to 12.11%, averaging 8.58%, and the average permeability is 0.302×10^{-3} μm^2 (Figure 3). The number of samples with porosity between 7.50% and 12.50% accounted for 75% of the total samples, showing extralow and low porosity. The permeability is mainly ultralow permeability. XRD results show that chlorite (48.84%) and illite (34.82%) are the main clay minerals, followed by the I/S mixed layer (16.35%) (Table 1). The areal porosity rate of low permeability sandstone samples averaged 2.1% (Table 2). Pore types mainly include intergranular pores, feldspar dissolved pores, lithic fragment dissolved pores, and intercrystalline pores (Table 2 and Figure 4). According to the distribution of porosity and permeability and mineral composition, 14 typical samples were selected to carry out the HPMI experiment, and 6 samples were selected to carry out the microscopic displacement model of real sandstone test.

3. Results and Discussions

3.1. Microscopic Pore Throat Structure. According to the results of HPMI data, the pore structure of Chang 6 reservoir in Wuqi area is divided into four types by pore structure parameters such as displacement pressure, median pressure, and maximum mercury saturation.

The displacement pressure of the type I pore structure is the lowest, less than 0.40 MPa, and the reservoir shows good physical properties, with an average porosity of 11.6% and permeability of 0.93×10^{-3} μm^2. The capillary pressure curve is mainly distributed in the lower left part (Table 3 and Figure 5). The pore types of type I are mainly intergranular pores and dissolution pores with large pore throat space, which is the best reservoir type in the study area. The displacement pressure of the type II pore structure is higher than that of type I, with an average of 0.67 MPa, and the porosity and permeability are lower than that of the type I pore structure. The capillary pressure curve is shifted upward to the right, but the flat section is longer than that of type I, indicating that the pore throat structure is relatively homogeneous (Table 3 and Figure 5). The pores of type II are mainly intergranular solution pores, and the seepage channel is mainly layered throat, which has good

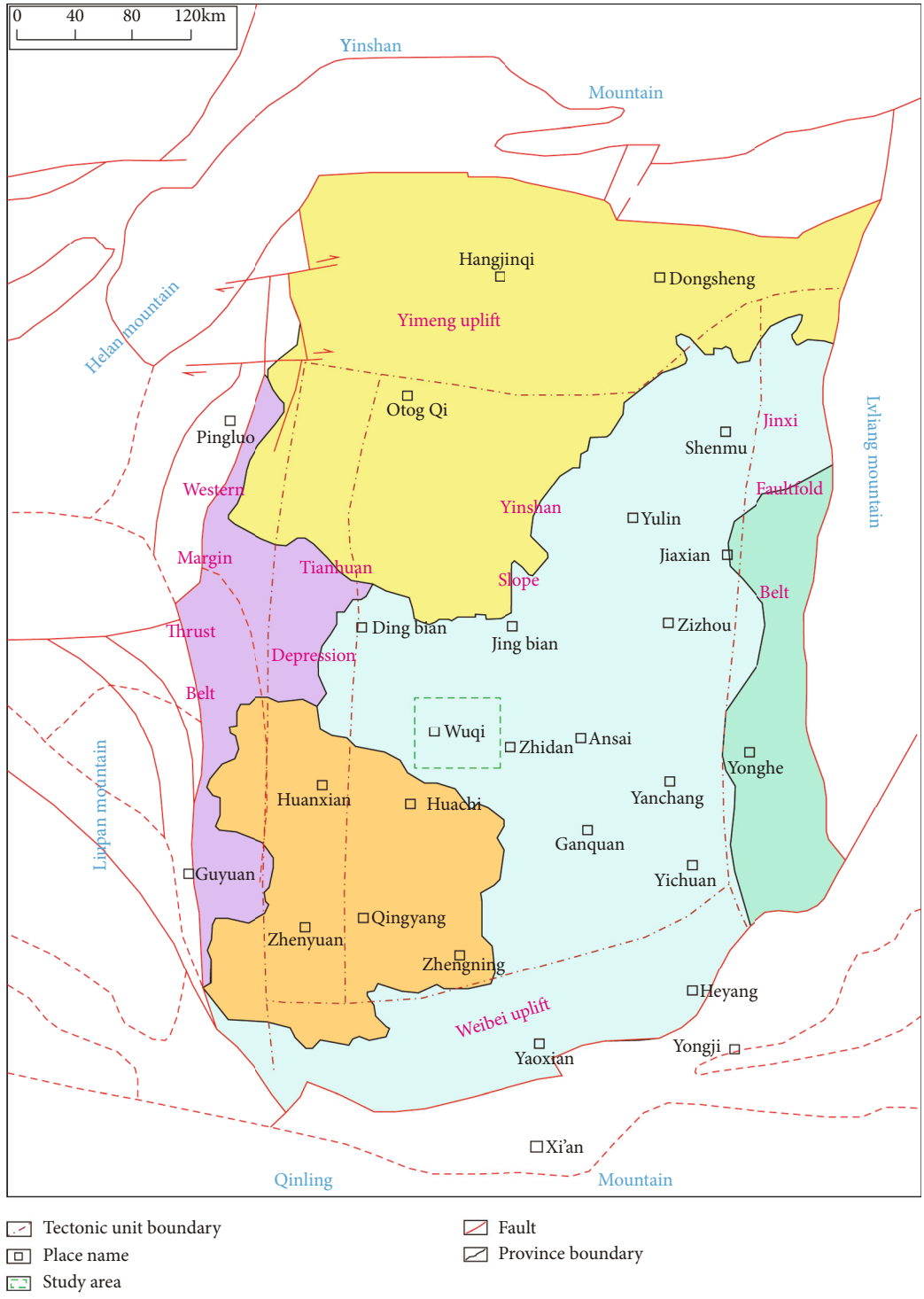

Figure 1: Geographical location of study area.

reservoir performance and seepage capacity, and is also the main type of further exploration and development in the study area.

The average displacement pressure of the type III pore structure is 1.16 MPa, and the average median radius is 0.07 μm. The capillary pressure curve shifted to the upper right, the displacement pressure is higher compared with type II, and the total mercury saturation of type III is low (Table 2 and Figure 5). The permeability of the type III reservoirs decreased significantly, with an average of 0.19×10^{-3} μm^2. The pore types are mainly dissolution pores and micropores, with small size throat and small pore throat space. The pores and throat configurations are poor, and the degree of heterogeneity is high. And the storage capacity

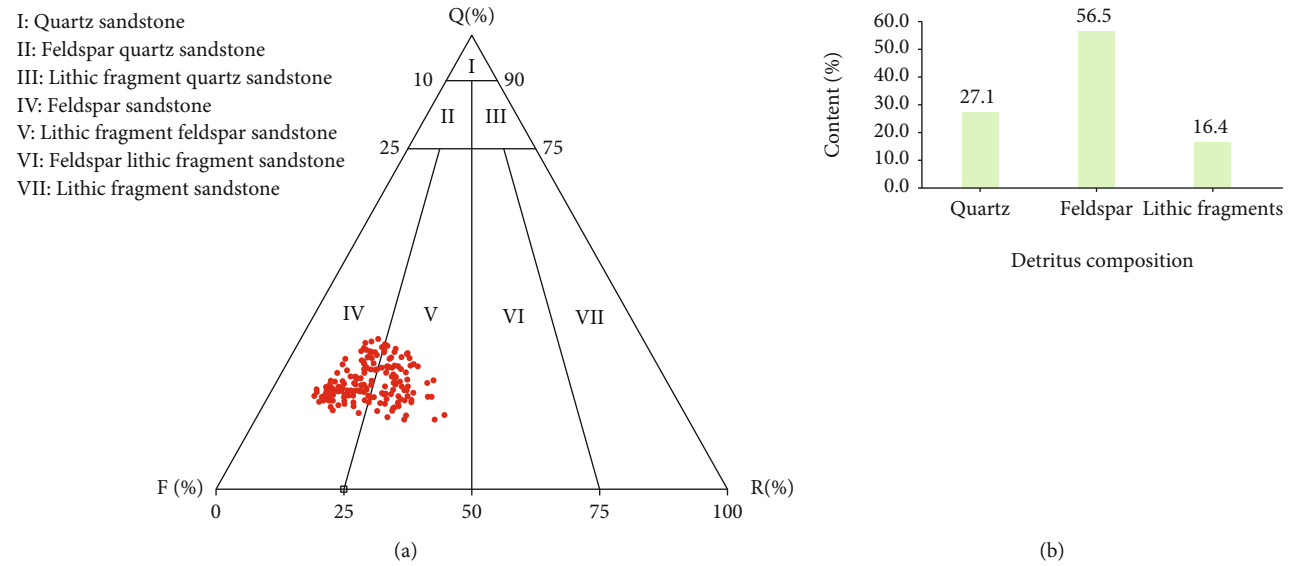

Figure 2: (a) Sandstone type distribution; (b) Detrital mineral composition distribution.

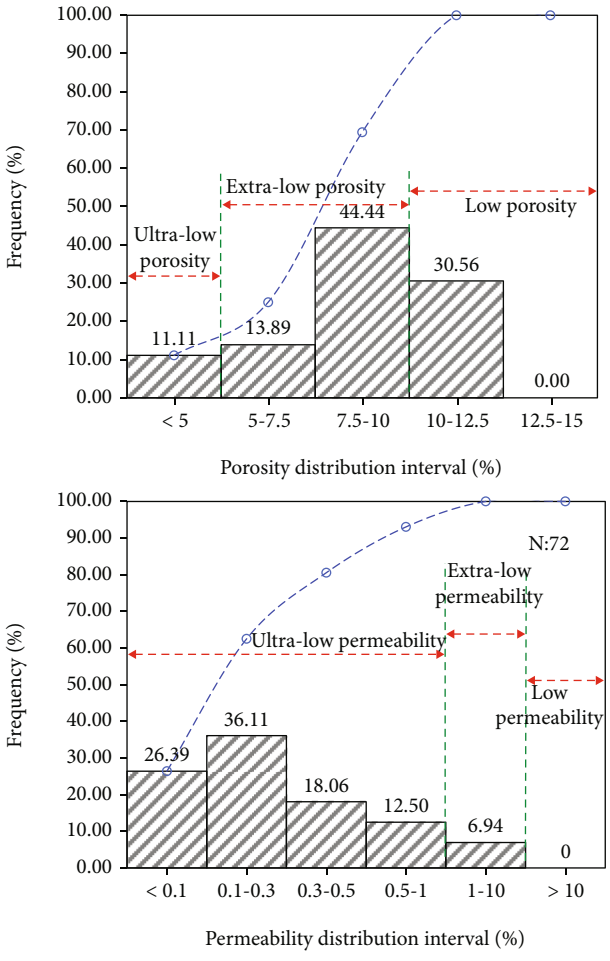

Figure 3: Histogram of reservoir physical property distribution.

and seepage capacity are poor. The type IV pore structures are the worst in the study area, with the highest displacement pressure (average 3.18 MPa), the smallest median radius (0.02 μm), and the lowest total mercury saturation (Table 3 and Figure 5). The type IV reservoirs have poor physical properties. The reservoir space is mainly intergranular pores of clay minerals, with good pore throat connectivity but poor seepage ability.

Table 1: Statistical table of clay mineral content.

Layer	Illite (%)	Chlorite (%)	Kaolinite (%)	I/S (%)	Total (%)
Chang 6	34.82	48.84	0.00	16.35	4.97

Maximum mercury saturation gradually decreased, and the displacement pressure increased from type I to type IV. Mercury saturation increases rapidly in the large pores of type I, and then, mercury is injected into the small pore throats uniformly. The pores and throats of type IV reservoirs are small, and there is no flat section of the capillary pressure curve. Mercury is injected into the pores and throats at a uniform rate. For low permeability reservoirs, the proportion of large pore throats is small, but the cumulative permeability contribution increases rapidly to about 98% within the large pore throat radius. The cumulative mercury saturation in this range also increases rapidly. Although the proportion of large pore throats is low, it is still the main storage space of the low permeability reservoir. As mercury gradually enters the small pore throat, the cumulative permeability contribution curve shows a gentle trend with a slow increase rate, but the increase rate of cumulative mercury saturation does not significantly decrease, indicating that permeability is still controlled by the large pore throat in the low permeability reservoir.

3.2. Characteristics of Different Types of Water Flooding. A microscopic displacement model of real sandstone experiments was carried out on typical samples of type I, type II, and type III. Table 4 shows the oil displacement efficiency

Table 2: Statistical table of proportion of pore types.

Layer	Intergranular pores (%)	Feldspar dissolved pores (%)	Lithic fragment dissolved pores (%)	Intercrystalline pores (%)	Microcracks (%)	Areal porosity rate (%)
Chang 6	1.4	0.4	0.1	0.1	0.0	2.1

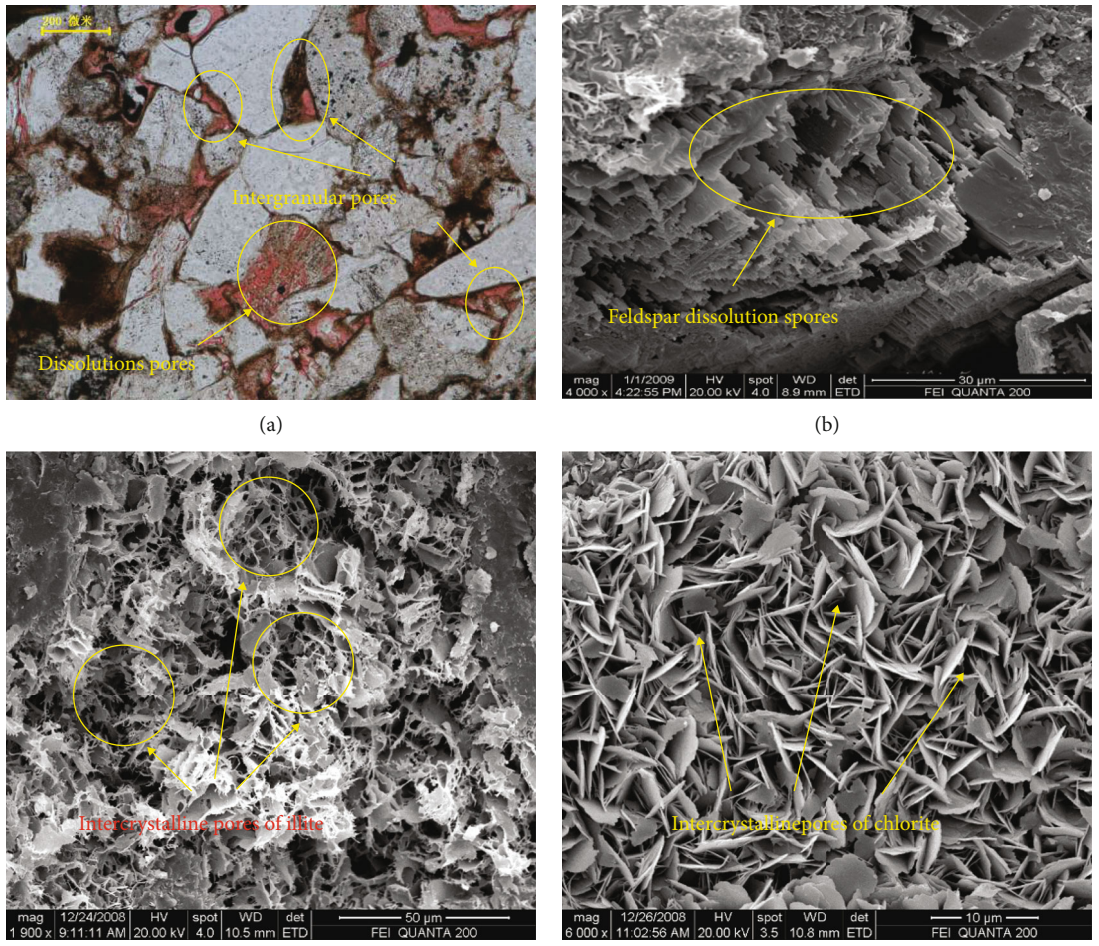

Figure 4: Microscopic pore types in Wuqi area: (a) intergranular pore X10, 1911.58 m; (b) the dissolution pore of feldspar X39, 1889.06 m; (c) intercrystalline pores of illite X20, 1879.18 m; (d) intercrystalline pores of chlorite X24, 1876.64 m.

statistics of 6 samples at different stages (Table 4). The final average oil displacement efficiency of the three types of samples is, respectively, 41.88%, 37.16%, and 30.00%, and the oil displacement efficiency gradually decreases with the deterioration of the reservoir pore structure. By studying the displacement types of water flooding in the process of water injection, it can be divided into uniform displacement (Figure 6(a)), mesh displacement (Figure 6(b)), and finger displacement (Figure 6(c)). The displacement effect of the three types is worse in turn.

The type I reservoir is dominated by uniform displacement, in which water moves evenly through the pores and throats, and in the process of water injection, water enters the pores under low pressure to replace oil. The displacement front is almost parallel, and there is no obvious hyperpermeability channel (Figure 6(a)). The swept area of water displacement increases gradually, and the displacement efficiency is high (Table 4). The oil displacement efficiency increments at different stages remained stable; for example, in samples X26 and X39, the oil displacement efficiency increment at the 2PV stage and 3PV stage was basically the same. The oil displacement efficiency of the type I reservoir is the highest, averaging 41.88%. Due to the good physical properties of the type I reservoir, the pore throat radius is larger, and the pore throat structure is relatively homogeneous. Water enters evenly from the middle of the pore and then extrudes oil from the surrounding, and the remaining oil is mainly attached to the pore throat surface in the form of oil film.

The type II reservoir is dominated by mesh type and partial finger displacement. In the process of water flooding, the

Table 3: Classification of pore structure parameters from HPMI.

Parameter type	Type I		Type II		Type III		Type IV	
	Distribution range	Average value	Distribution range	Average value	Distribution range	Average value	Distribution range	Average value
Porosity (%)	11.16~12.11	11.6	8.98~11.50	9.9	8.97~9.01	8.99	4.99~10.43	7.84
Permeability ($\times 10^{-3}$ μm^2)	0.69~1.09	0.93	0.21~0.72	0.39	0.17~0.21	0.19	0.04~0.19	0.11
Displacement pressure (MPa)	0.29~0.46	0.35	0.45~0.74	0.67	1.14~1.17	1.16	1.82~4.49	3.08
Maximum mercury saturation (%)	87.45~90.02	88.71	85.10~92.43	88.17	83.25~87.89	86.17	71.92~87.80	81.85
Median radius (μm)	0.08~0.22	0.16	0.07~0.20	0.13	0.05~0.12	0.07	0.01~0.03	0.02
Maximum pore throat radius (μm)	1.60~2.54	2.22	0.99~1.62	1.13	0.63~0.64	0.64	0.16~0.40	0.27
Sorting coefficient	2.40~2.91	2.61	1.81~2.46	2.28	2.22~2.54	2.4	2.01~3.55	2.64
Mean coefficient	10.32~10.73	10.53	10.62~11.51	10.98	10.50~11.75	11.29	10.01~13.26	11.88
Proportion	21.00%		36.00%		21.00%		21.00%	

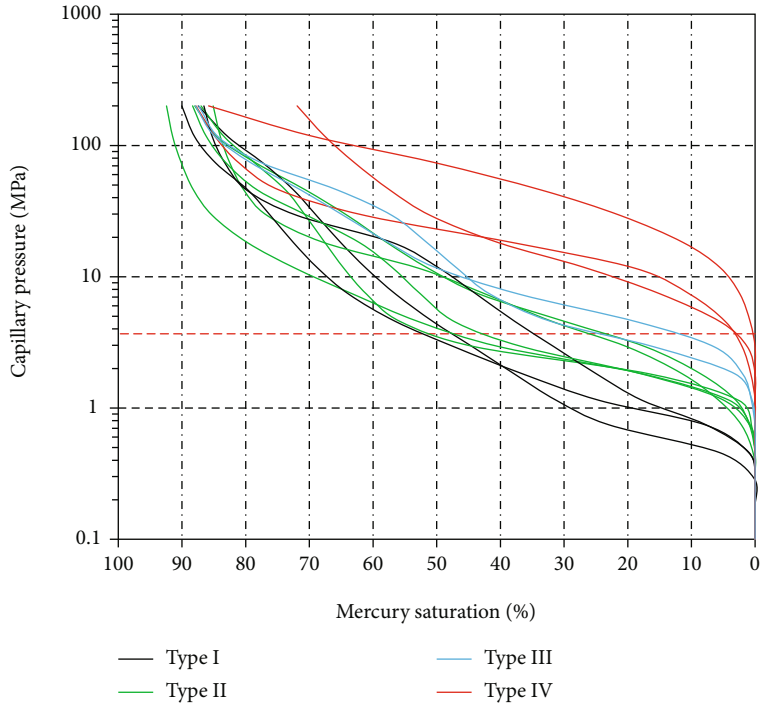

Figure 5: The capillary curves of HPMI.

Table 4: Microscopic displacement model of real sandstone test parameters.

Type	Well	Depth (m)	Displacement type	Average oil displacement efficiency (%)	Displacement multiple				
					1PV	2PV		3PV	
					Oil displacement efficiency (%)	Oil displacement efficiency (%)	Displacement efficiency increment (%)	Oil displacement efficiency (%)	Displacement efficiency increment (%)
I	X26	1880.50	Uniform displacement	41.88	33.49	40.93	7.44	46.51	5.58
	X39	1884.57			28.96	33.85	4.89	37.25	3.40
II	X9	1829.87	Mesh displacement	37.16	33.17	39.02	5.85	40.98	1.95
	X19	1784.71			20.00	30.00	10.00	33.33	3.33
III	X27	1823.20	Finger displacement	30.00	17.78	29.63	11.85	35.56	5.93
	X28	1910.85			13.33	22.22	8.89	24.44	2.22

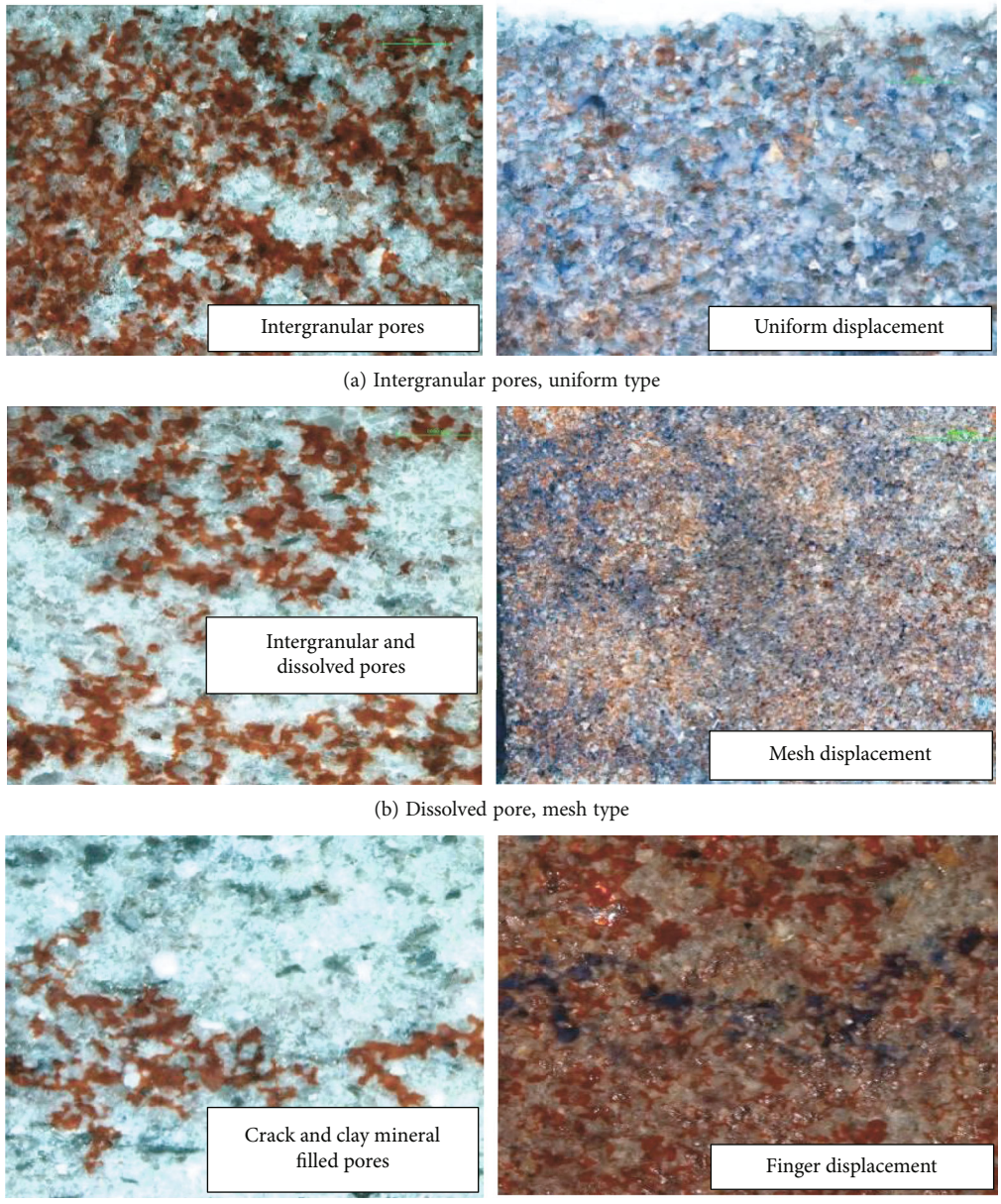

(a) Intergranular pores, uniform type

(b) Dissolved pore, mesh type

(c) Cracks and clay mineral filled pores, finger type

Figure 6: Different water displacement types.

oil displacement efficiency increases rapidly in the early stage with a small increment in the later stage (Table 4). Due to the relatively complex pore throat structure of the type II reservoir, water firstly enters the large pores with relatively small pore resistance, resulting in a fingering phenomenon, so the oil displacement efficiency increases rapidly in the early stage of oil displacement. At the later stage of displacement, with the increase of water injection pressure, water enters the small pore throats; the oil displacement efficiency increases slowly and gradually forms a mesh seepage channel. Due to the good connectivity between the small pore throats, mesh uniform displacement is formed in the later stage. The average displacement efficiency of the type II reservoir is 37.16%, which is mainly contributed by the large pore throat, and the displacement rate of the large pore throat is obviously higher than that of the small pore throat. If the displacement rate in the large pore throat is higher than that in the small pore throat, the oil discharged from the small pore throat is captured by the water in the large pore throat, forming a water lock phenomenon. If the displacement rate of the small pore throat is faster than that of the large pore throat, the oil in the large pore throat will be separated and surrounded by the water in the small pore throat, forming oil droplets. The remaining oil of the type II reservoir mainly consists of water blocking and oil drop.

Type III reservoirs have low displacement efficiency, averaging only 30.00%. In the displacement process, water moves forward in a finger shape along the high permeability zone, which is mainly due to the poor physical property,

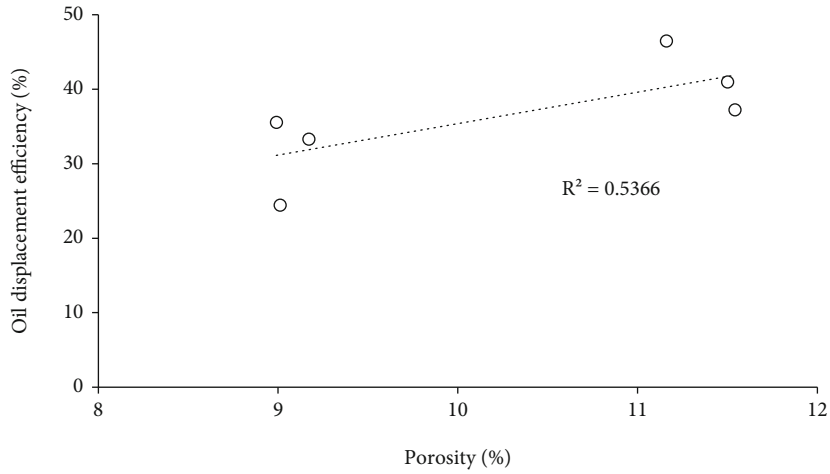

(a) Porosity vs. displacement efficiency

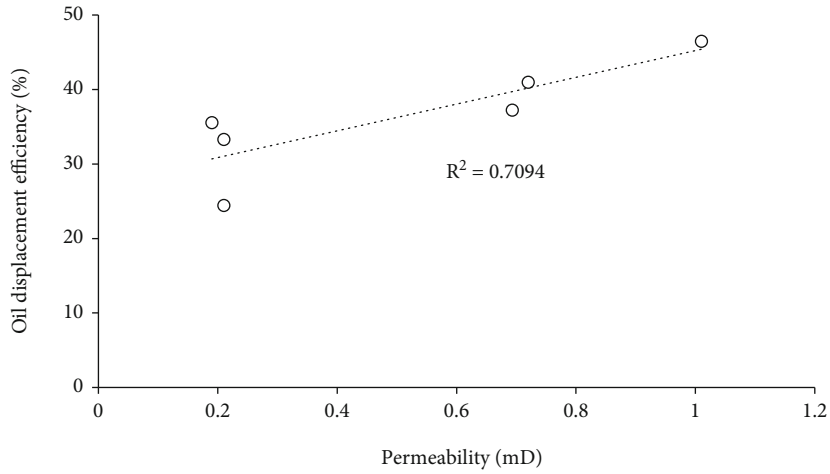

(b) Permeability vs. displacement efficiency

Figure 7: Correlation between displacement efficiency and physical properties.

poor connectivity, and complex structure of the reservoir. Water can only enter a few pores and throats under a certain pressure, presenting a finger-forward phenomenon, and the water injection area is dispersed. The type III reservoir has a short stable production period and low recovery factor. The reservoir is easy to form contiguous remaining oil due to its small pore throat radius, high pore throat blockage rate, and narrow water injection sweep area (Figure 6(c)). Due to the small pore throat and complex structure of the type IV reservoir samples, most of them are invalid reservoirs, so the microscopic displacement model of real sandstone experiments has not been carried out.

3.3. Influencing Factors of Displacement Efficiency

3.3.1. Correlation between Displacement and Reservoir Physical Properties. To some extent, reservoir physical property is an intuitive parameter reflecting pore throat structure, especially the variation of permeability, which can directly represent the ability of pore throat to fluid flow. By analyzing the relationship between physical parameters of samples with different pore throat structures and displacement efficiency, it can be seen that there is a positive correlation between porosity, permeability, and the final oil displacement efficiency, and the correlation coefficient (R^2) is 0.5366 and 0.7094, respectively (Figures 7(a) and 7(b)). The positive correlation between permeability and the final oil displacement efficiency is more obvious. It indicates that the better pore throat configuration and connectivity of samples, the stronger reservoir seepage capacity and the higher oil displacement efficiency. However, for the low permeability reservoir, the pore throat radius is small, the connectivity is poor, the configuration is complex, and there are problems of high permeability, low oil displacement efficiency, and low permeability and high oil displacement efficiency. The reservoir physical property still has certain limitations in the aspect of reaction oil displacement efficiency, and the seepage capacity cannot effectively control the oil displacement efficiency.

3.3.2. Effects of the Different Pore Throat Structures on Displacement Efficiency. The pore throat structure of the four types of reservoirs is different, and the dominant pore types of each type are different. The content and distribution

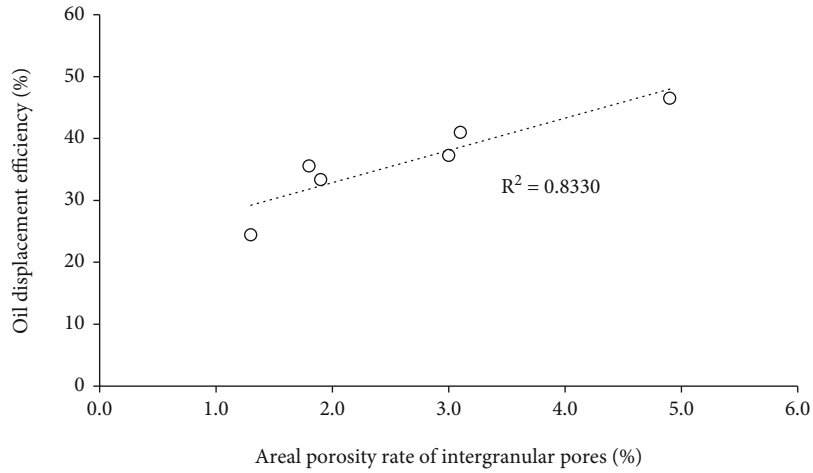

(a) Areal porosity rate of intergranular pores vs. displacement efficiency

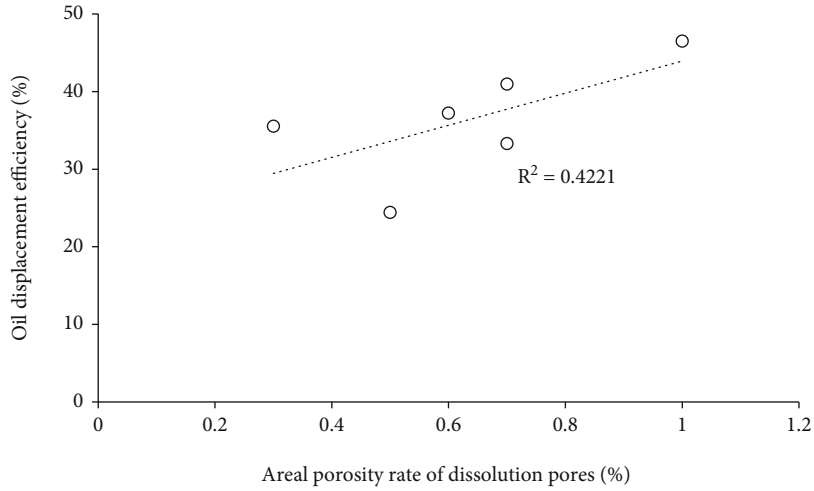

(b) Areal porosity rate of dissolution pores vs. displacement efficiency

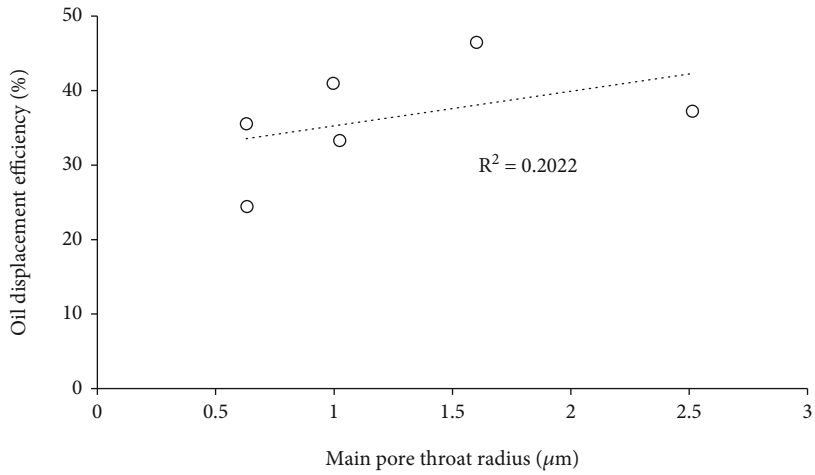

(c) Main pore throat radius vs. displacement efficiency

Figure 8: Continued.

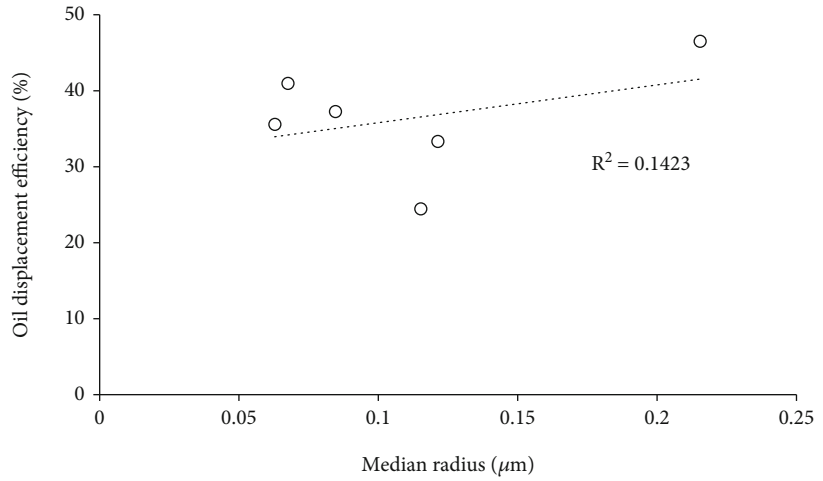

(d) Medium radius vs. displacement efficiency

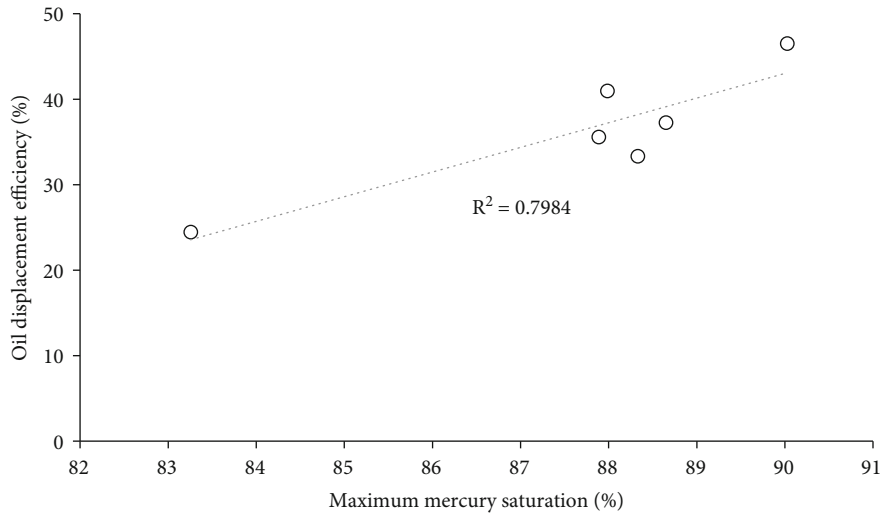

(e) Maximum mercury saturation vs. displacement efficiency

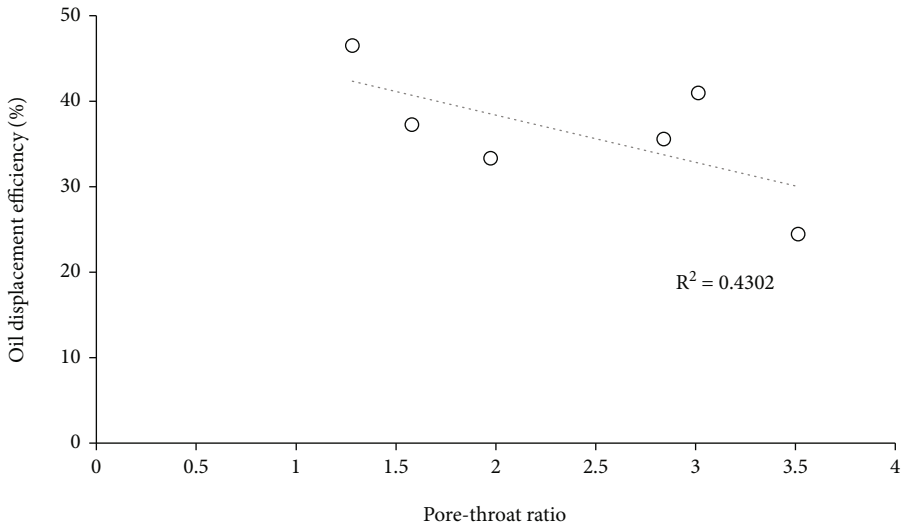

(f) Pore-throat ratio vs. displacement efficiency

Figure 8: Correlation between pore structure parameters and displacement efficiency.

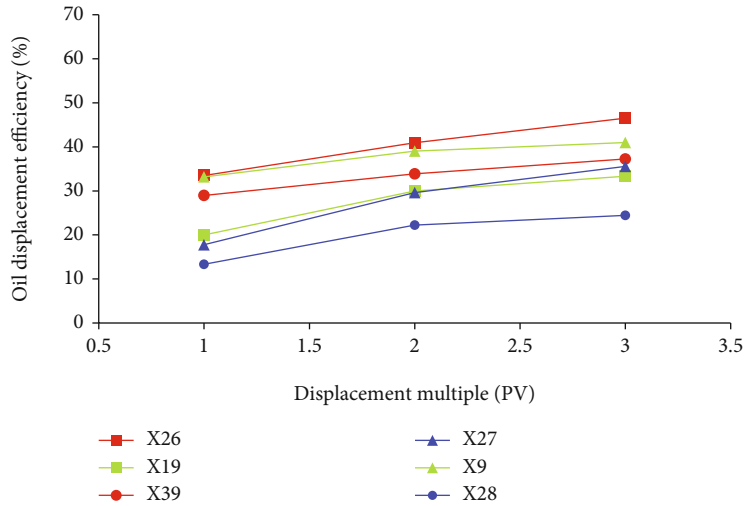

Figure 9: Displacement efficiency under different volume displacement multiples.

of clay minerals in different pore types are different, resulting in different displacement efficiency. According to the relationship between the statistical results of pore types in cast thin slices of different reservoir types and displacement efficiency, it can be obtained (Figures 8(a) and 8(b)) that the higher the intergranular areal porosity ratio is, the better the displacement efficiency is. There is also a positive correlation between dissolution pores and displacement efficiency. The reservoir dominated by intergranular pores has higher oil displacement efficiency, and the displacement path is mainly uniform type and mesh type, and the sweep range is generally wide. The displacement efficiency of the reservoir dominated by dissolution pores is lower than that of the intergranular pore type and is dominated by mesh and finger displacement. This type of reservoir has a high permeability zone, so the oil displacement efficiency is very high at 1PV but increases slowly when it increases to 3PV. The reservoir dominated by micropores has the lowest oil displacement efficiency. As the pores are mostly filled by interstitial materials such as clay minerals, the pores become smaller or blocked, so they are mostly micropores between clay minerals. Therefore, with the increase of displacement multiple, displacement efficiency does not improve significantly.

The pore throat structure is the key factor affecting displacement efficiency in low permeability reservoirs. The larger the pore throat, the larger the storage space of fluid, and the more homogeneous samples with a large pore throat, the stronger the percolation ability of fluid in the pore throat space. According to the relationship between HPMI pore throat structure parameters and the displacement efficiency, the main pore throat radius and median pore throat radius and the displacement efficiency have a weak positive correlation between (Figures 8(c) and 8(d)), but the correlation is not obvious; this is due to the pore structure of low permeability reservoir being complex; the main pore throat and median pore throat radius do not represent the overall pore throat structure of the sample. There is a significant positive correlation between the maximum mercury saturation and displacement efficiency (Figure 8(e)). The larger the maximum mercury saturation is, the larger the pore throat space of the sample is, and the pore throat structure is conducive to fluid flow, and the corresponding displacement efficiency is also higher. There is a negative correlation between the pore throat ratio and displacement efficiency (Figure 8(f)). The larger the pore throat ratio is, the more inhomogeneous the pore throat structure is, and the lower the displacement efficiency is. It can be seen that pore throat size and homogenization are important factors affecting oil displacement efficiency. The size of the pore throat has good control on water flooding efficiency. With the increase of pore throat radius, the permeability of fluid in the reservoir increases, the diffusion range of fluid expands, and the oil displacement efficiency increases. The more inhomogeneous the pore throat structure is, the more likely is fluid to move along the high permeability channel, resulting in a large number of bypassing phenomena, which causes a large amount of oil to stay in the pores, resulting in a significant decrease in oil displacement efficiency.

3.3.3. Displacement Characteristics. The displacement efficiency of different types of pore throat structures under different volume displacement multiples was analyzed. With the increase of volume displacement multiples, the displacement efficiency also increased. Generally, the increase rate of displacement efficiency decreases with the increase of volume displacement multiple. For example, the displacement efficiency of type II reservoir and type III reservoir varies greatly within 1PV-2PV volume displacement multiple. When volume displacement multiple reaches 3PV, it can be found that the increase rate of displacement efficiency decreases significantly and gradually changes significantly (Figure 9). However, the increase rate of displacement efficiency remains stable under different volume displacement multiples, indicating that the pore throat structure of the type I reservoir is better. In the actual water injection process, increasing volume displacement multiple in a certain range can improve the sweep area and displacement efficiency. When displacement multiple is too high, movable

fluid saturation will decrease, resulting in lower oil displacement efficiency, which is often counterproductive [19]. Therefore, actual water injection development, through the formulation of appropriate and reasonable water injection volume multiple, can better achieve the purpose of enhanced oil recovery.

Through the displacement experiment in the study area, it is found that the complex and small pore structure of the low permeability sandstone reservoir leads to a slow water flooding process. As displacement pressure increases, displacement efficiency also increases. With the increase of displacement pressure, the water that originally moved along the large pore and high permeability zone overcame the capillary force in the small pore throat and gradually moved to the relatively low permeability zone, thus improving the oil displacement efficiency.

4. Conclusions

The rock types of Chang 6 low permeability sandstone reservoir in Wuqi area of Ordos Basin are mainly feldspar sandstone and lithic feldspar sandstone, and the main detrital minerals are quartz, feldspar, and lithic. The clay minerals are mainly chlorite, illite, and I/S mixed layer. The areal porosity rate of low porosity samples averaged 2.1%, and the average porosity is 8.58%, with extralow pores. The average permeability is $0.302 \times 10^{-3}\ \mu m^2$, and the permeability is mainly ultralow. The pore types mainly include intergranular pores and feldspar dissolution pores.

According to the HPMI and image results, the pore throat types in the study area were classified into four types. From type I to type IV, the maximum mercury saturation and median radius gradually decreased, the pore throat structure gradually deteriorated, and the corresponding displacement efficiency also gradually decreased. The displacement efficiency of the type I reservoir is the highest, which is dominated by uniform displacement, and the remaining oil is dominated by oil film type. The displacement efficiency of the type II reservoir is lower than that of type I, which is dominated by mesh and finger displacement, and the residual oil is dominated by water-locked and droplets. The type III reservoir has the worst displacement efficiency and is dominated by finger displacement, which is easy to form contiguous remaining oil distribution after water displacement.

There is an obvious positive correlation between displacement efficiency and permeability in Wuqi area, and the stronger the seepage capacity, the higher the oil displacement efficiency. Pore throat size and homogenization are important factors affecting oil displacement efficiency. With the increase of pore throat radius, the permeability of fluid in the reservoir increases, the diffusion range of fluid expands, and the oil displacement efficiency increases. The increase rate of displacement efficiency remains stable under different volume displacement multiples, indicating that the pore throat structure of the type I reservoir is better. The increase rate of displacement efficiency decreases with the increase of volume displacement multiple of type II and III reservoirs. In the actual water flooding development process, the higher displacement pressure is not the better, and reasonable control of displacement pressure is the key to production growth.

Data Availability

The data used to support the findings of this study are available from the corresponding author upon request.

Additional Points

Highlights. According to the HPMI, the pore throat types were classified into four types. From type I to type IV, the size and homogeneity of the pore throat structure deteriorate gradually, and the corresponding displacement efficiency also gradually decreased. Pore throat size and homogenization are important factors affecting oil displacement efficiency. The displacement efficiency of different types of pore throat structures under different volume displacement multiples was analyzed, and the more stable the growth rate of displacement efficiency, the better the pore throat structure.

Conflicts of Interest

The authors declare that they have no conflicts of interest.

References

[1] J. Chengzao, M. Zheng, and Y. Zhang, "Unconventional hydrocarbon resources in China and the prospect of exploration and development," *Petroleum Exploration and Development*, vol. 39, no. 2, pp. 139–146, 2012.

[2] C. N. Zou, S. Z. Tao, and Z. Yang, "New advance in unconventional petroleum exploration and research in China," *Bulletin of Mineralogy, Petrology and Geochemistry*, vol. 31, no. 4, pp. 312–322, 2012.

[3] R. Zhu, C. Zou, Z. Mao et al., "Characteristics and distribution of continental tight oil in China," *Journal of Asian Earth Sciences*, vol. 178, pp. 37–51, 2019.

[4] C. N. Zou, S. Z. Tao, X. J. Yuan, R. K. Zhu, D. Z. Dong, and W. Li, "Global importance of "continuous" petroleum reservoirs: accumulation, distribution and evaluation," *Petroleum Exploration and Development*, vol. 36, no. 6, pp. 669–682, 2009.

[5] H. Yang, J. Fu, H. He, X. Liu, Z. Zhang, and X. Deng, "Formation and distribution of large low-permeability lithologic oil regions in Huaqing, Ordos Basin," *Petroleum Exploration ang Development*, vol. 39, no. 6, pp. 683–691, 2012.

[6] J. Fu, X. Deng, Q. Wang, J. Qiu, W. Hao, and Y. Zhao, "Densification and hydrocarbon accumulation of Triassic Yanchang Formation Chang 8 Member, Ordos Basin, NW China: evidence from geochemistry and fluid inclusions," *Petroleum Exploration ang Development*, vol. 44, no. 1, pp. 48–57, 2017.

[7] J. H. Fu, J. Yu, L. M. Xu, X. B. Niu, S. B. Feng, and X. J. Wang, "New progress in exploration and development of tight oil in Ordos Basin and main controlling factors of largescale enrichment and exploitable capacity," *China Petroleum Exploration*, vol. 20, no. 5, pp. 9–19, 2015.

[8] R. G. Loucks, R. M. Reed, S. C. Ruppel, and D. M. Jarvie, "Morphology, genesis, and distribution of nanometer-scale pores in

siliceous mudstones of the Mississippian Barnett Shale," *Journal of Sedimentary Research*, vol. 79, no. 12, pp. 848–861, 2009.

[9] D. Ren, D. Zhou, D. Liu, F. Dong, S. Ma, and H. Huang, "Formation mechanism of the Upper Triassic Yanchang Formation tight sandstone reservoir in Ordos Basin–take Chang 6 reservoir in Jiyuan oil field as an example," *Journal of Petroleum Science and Engineering*, vol. 178, pp. 497–505, 2019.

[10] D. K. Liu, D. Z. Ren, K. Du, Y. R. Qi, and F. Ye, "Impacts of mineral composition and pore structure on spontaneous imbibition in tight sandstone," *Journal of Petroleum Science and Engineering*, vol. 201, article 108397, 2021.

[11] L. M. Anovitz and D. R. Cole, "Characterization and analysis of porosity and pore structures," *Reviews in Mineralogy &Geochemistry*, vol. 80, no. 1, pp. 61–164, 2015.

[12] Y. Q. Qu, W. Sun, R. D. Tao, B. Luo, L. Chen, and D. Z. Ren, "Pore-throat structure and fractal characteristics of tight sandstones in Yanchang Formation, Ordos Basin," *Marine and Petroleum Geology*, vol. 120, p. 104573, 2020.

[13] D. Z. Ren, T. Li, D. Liu, J. Tao, X. Liu, and R. Zhang, "Control mechanism and parameter simulation of oil-water properties on spontaneous imbibition efficiency of tight sandstone reservoir," *Frontiers in Physics*, vol. 176, no. 10, article 829763, 2022.

[14] Y. R. Guo, J. B. Liu, H. Yang, Z. Liu, J. H. Fu, and J. L. Yao, "Hydrocarbon accumulation mechanism of low permeable tight lithologic oil reservoirs in the Yanchang Formation Ordos Basin, China," *Petroleum Exploration and Development*, vol. 39, no. 4, pp. 417–425, 2012.

[15] Y. Q. Qu, W. Sun, H. N. Wu et al., "Impacts of pore-throat spaces on movable fluid: implications for understanding the tight oil exploitation process," *Marine and Petroleum Geology*, vol. 137, article 105509, 2022.

[16] X. Huang, T. T. Li, X. Z. Wang, H. Gao, and J. Ni, "Distribution characteristics and its influence factors of movable fluid in tight sandstone reservoir: a case study from Chang 8 oil layer of Yanchang Formation in Jiyuan Oilfield Ordos Basin," *Acta Petrolei Sinica*, vol. 40, no. 5, pp. 557–567, 2019.

[17] J. J. Zhou, "Characteristics of the pore-throat structures and their influences on the waterflooded oil micro-features for Chang 8 reservoir in Pingbei block of Yanchang Oilfield," *Petroleum Geology and Oilfield Development in Daqing*, vol. 36, no. 5, pp. 68–79, 2017.

[18] D. Z. Ren, H. P. Zhang, Z. Z. Wang, B. Y. Ge, D. K. Liu, and R. J. Zhang, "Experimental study on microscale simulation of oil accumulation in sandstone reservoir," *Frontiers in Physics*, vol. 10, article 841989, 2022.

[19] X. Zhang, D. Z. Ren, Q. Y. Ren, H. Huang, D. K. Liu, and X. F. Qu, "The feature of the microscopic pore structure and its influence on oil displacement efficiency in Chang 6 reservoir in Jiyuan Oilfield of Ordos Basin," *Journal of Northwest University (Natural Science Edition)*, vol. 45, pp. 283–290, 2015.

[20] M. Shabaninejad, J. Middleton, S. Latham, and A. Fogden, "Pore-scale analysis of residual oil in a reservoir sandstone and its dependence on water flood salinity, oil composition, and local mineralogy," *Energy & Fuels*, vol. 31, no. 12, pp. 13221–13232, 2017.

[21] F. Zhang, W. Sun, X. Zhang, B. Hu, M. Ma, and B. Wang, "The application of electron microscope in the oilfield development: in the case of Chang 6 reservoir in Ban Qiao-He Shui area," *Journal of Chinese Electron Microscopy Society*, vol. 36, no. 4, pp. 358–369, 2017.

[22] L. M. Anovitz, D. R. Cole, G. Rother, L. F. Allard, A. J. Jackson, and K. C. Littrell, "Diagenetic changes in macro- to nano-scale porosity in the St. Peter Sandstone: an (ultra) small angle neutron scattering and backscattered electron imaging analysis," *Geochimica et Cosmochimica Acta*, vol. 102, pp. 280–305, 2013.

[23] C. R. Clarkson, M. Freeman, L. He et al., "Characterization of tight gas reservoir pore structure using USANS/SANS and gas adsorption analysis," *Fuel*, vol. 95, pp. 371–385, 2012.

[24] R. F. Wang and W. Sun, "Main controls for oil displacement efficiency by the micro model water flooding experiment in ultra-low permeability sandstone reservoir," *Petroleum Geology & Experiment*, vol. 32, no. 1, pp. 93–97, 2010.

[25] H. H. Quan, Y. S. Zhu, H. J. Zhang, L. Li, F. Shao, and Z. Zhang, "Reservoir pore structure and micro-flow characteristics of waterflooding: a case study from Chang 6 reservoir of Wangyao block in Ansai Oilfield," *Oil & Gas Geology*, vol. 32, no. 54, pp. 952–964, 2011.

[26] H. Huang, L. Chen, W. Sun et al., "Pore-throat structure and fractal characteristics of Shihezi Formation tight gas sandstone in the Ordos Basin, China," *China Fractals*, vol. 26, no. 2, p. 1840005, 2018.

[27] D. Liu, Z. Gu, R. Liang et al., "Impacts of pore-throat system on fractal characterization of tight sandstones," *Geofluids*, vol. 2020, Article ID 4941501, 17 pages, 2020.

[28] E. W. Washburn, "The dynamics of capillary flow," *American Physical Society*, vol. 17, no. 3, pp. 273–283, 1921.

[29] W. R. Purcell, "Capillary pressures - their measurement using mercury and the calculation of permeability therefrom," *Journal of Petroleum Technology*, vol. 1, no. 2, pp. 39–48, 1949.

[30] S. M. Hassanizadeh, M. A. Celia, and H. K. Dahle, "Dynamic effect in the capillary pressure–saturation relationship and its impacts on unsaturated flow," *Vadose Zone Journal*, vol. 1, no. 1, pp. 38–57, 2002.

[31] J. Lai and G. Wang, "Fractal analysis of tight gas sandstones using high-pressure mercury intrusion techniques," *Journal of Natural Gas Science and Engineering*, vol. 24, pp. 185–196, 2015.

[32] H. Gao, W. Xie, J. P. Yang, C. Zhang, and W. Sun, "Pore throat characteristics of extra-ultra-low permeability sandstone reservoir based on constantrate mercury penetration technique," *Petroleum Geology & Experiment*, vol. 33, no. 2, pp. 206–211, 2011.